ChemComm

Accepted Manuscript

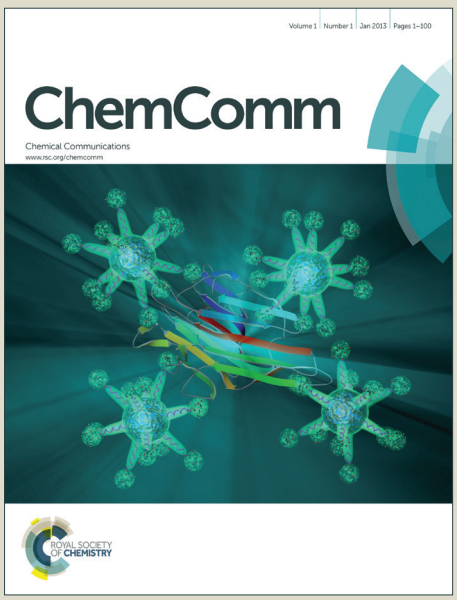

ROYAL SOCIETY OF CHEMISTRY

www.rsc.org/chemcomm

ChemComm

COMMUNICATION

Chromium nitride /carbon nanocapsules containing carbon nitride hybrid as Pt-free electrocatalyst for oxygen reduction

Received 00th January 20xx,
Accepted 00th January 20xx

DOI: 10.1039/x0xx00000x

www.rsc.org/

Lu Zhao, Lei Wang,* Peng Yu, Dongdong Zhao, Chungui Tian, He Feng, Jing Ma and Honggang Fu*

Chromium nitride nanoparticles supported on graphitic carbon nanocapsules (CrN/GC) containing carbon nitrides hybrid has been synthesized by a solvothermal-assisted ion-exchanged route. As Pt-free catalyst, the CrN/GC hybrid exhibits superior activity, stability, methanol immune and a dominant 4-electron pathway towards oxygen reduction reaction.

Fuel cells (FCs) are promising energy conversion devices for exploration of renewable alternative energies.[1] In comparison with the oxidation reaction at anode (especially hydrogen fuel), the cathodic oxygen reduction reaction (ORR) is the bottleneck owing to its sluggish kinetics.[2] The ideal catalyst should meet the requirements of low overpotential and four-electron reduction pathway.[3] Pt-based catalysts, including alloy and special morphologies, are currently the most effective ORR catalysts with the lowest overpotential and a direct four-electron reduction path.[4] However, the high cost, scarce supply and fuel crossover effect of Pt have severely hindered its large-scale commercial applications. Consequently, extensive research efforts have been undertaken to develop non-precious metal catalysts based on sustainable and abundant elements but also with high ORR activity and superior stability.[5]

In this respect, a various of catalysts based on non-precious metal complexes (Fe, Co, Ni-based oxides, carbides or phosphides, *etc*.),[6] doping carbon materials (N, S and P single- or multiple-doped mesoporous carbon, carbon nanotubes, graphene materials, carbon nitride *etc*.) have been extensively studied.[7-11] Alternatively, transition metal nitrides (TMNs) have been established the most promising candidates for replacing Pt catalyst due to the precious metal-like property, which is ascribed from their electronic structures similar to the precious metals. Moreover, TMNs possess highly electronic conductivity, excellent thermal stability, exceptional hardness and corrosion resistance under FCs operation.[12] To date, Fe_xN, CoN, TiN, WN and MoN have been studied intensively.[13] As for the same family and periodic element shows the similar properties, it arouses us consider the chromium nitride (CrN) would exhibit ORR activity. Unfortunately, although CrN as support for Pt catalyst towards anodic electrooxidation has been reported,[14] the relative study about ORR is scare. Various synthetic approaches have been used for preparing CrN-based materials, including vapor deposition, plasma nitridation, sputtering, templating, nanopatterning electrochemical route, *etc*.[15] Nevertheless, most of them suffer from the rigorous synthetic conditions of high temperatures, air-sensitive or toxic reagents, resulting in the limitation of large-scale commercial application.[16] Based on this situation, it is highly desirable to propose a simple and efficiency strategy for synthesis of CrN-based nanostructures with well ORR performance.

Herein, we demonstrate a novel CrN/ graphitic carbon nanocapasules (CrN/GC) hybrid containing carbon nitrides as electrocatalyst obtained from a simple solvothermal-assisted ion-exchanged route. In the synthesis, the low-cost polyacrylic weak-acid anion-exchanged resin (PWAR) has uniform skeleton and exchangeable groups, which could make functional ions well disperse and strongly embed. The $Cr_2O_7^{2-}$ and $[Fe(CN)_6]^{3-}$ ions as the resources of CrN and graphitic catalyst, respectively, are introduced into the backbone of PWAR through an ion-exchanged process and a subsequent solvothermal. After a nitridation process and then treating with hydrochloric acid, the CrN/GC hybrid could be obtained (see experimental section, Table S1 and Scheme S1 in the supporting information). The existence of GC in hybrid can contributes to the high electrocatalytic activity, because they can assist in both dispersing the metal catalysts and dominating electron transfer, facilitating mass transport kinetics at the electrode surface. The synthetic CrN/GC hybrid is used as ORR catalyst for the first time and shows excellent electrocatalytic activity for ORR in alkaline medium, including higher diffusion limiting current density, excellent methanol immune, well durability and a four-electron pathway.

X-ray diffraction (XRD) pattern of the synthetic CrN/GC-2-900 hybrid derived from 0.05 M $Cr_2O_7^{2-}$ with a carbonized temperature of 900 °C exhibits a characteristic peak at 26.4°

Laboratory of Functional Inorganic Material Chemistry, Ministry of Education of the People's Republic of China, Heilongjiang University, Harbin 150080, P. R. China
E-mail: fuhg@vip.sina.com; Tel: 0451-86604330
Electronic Supplementary Information (ESI) available: experimental details and charaterizations. See DOI: 10.1039/x0xx00000x

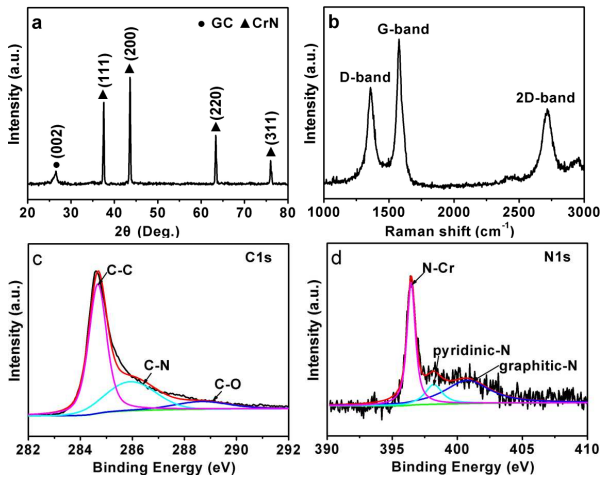

Fig. 1 (a) XRD pattern and (b) Raman spectrum of the CrN/GC-2-900 hybrid; (c) high-resolution (c) C1s and (d) N1s XPS spectra of the CrN/GC-2-900 hybrid.

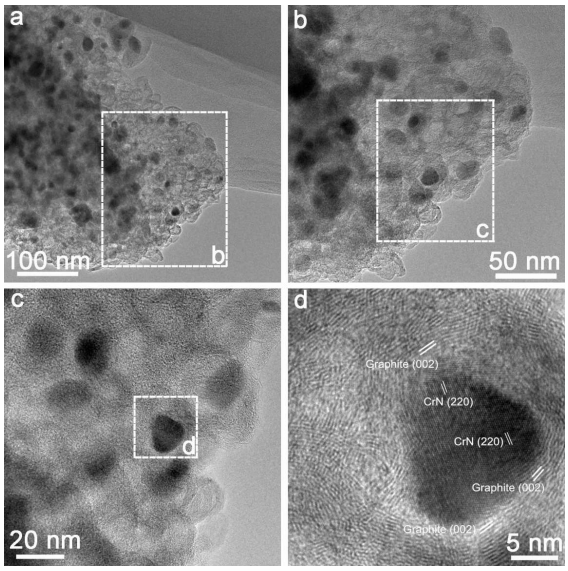

Fig. 2 TEM and HRTEM images of CrN/GC-2-900 hybrid.

corresponding to GC(002) plane, and the other four peaks are matched well with the diffraction peaks of CrN (JCPDS 03-065-2899) (Fig. 1a), confirming the formation of CrN/GC. The Raman spectrum of CrN/GC-2-900 shows the narrow D-band at 1355 cm^{-1} and G-band at 1574 cm^{-1}, companying with the intense 2D-band at 2723 cm^{-1}, which are the characterizations of the graphitic carbon with high crystallinity. The intensity ratio of I_G/I_D is about 1.43, implying a well electron conductivity of the hybrid, which is benefit to the electron transfer during ORR. The GC sample synthesized from the same process as that of CrN/GC-2-900 only in the absence of $Cr_2O_7^{2-}$ (Table S1 and Fig. S3) was also prepared for comparison. It can be seen that the I_G/I_D value for CrN/GC-2-900 is lower than that of GC (about 1.82) as shown in Fig S3b. Such phenomenon is attributed to the formation of CrN would prevent the crystalline of graphitic carbon. The CrN weigh content in the hybrid is about 50.7 % tested by the TG curve (see Fig. S1 and Table S2).

Wide X-ray photoelectron spectroscopy (XPS) analysis in Fig. S2 reveals the CrN/GC-2-900 is mainly composed of C, N, O and Cr elements. Deconvolution of the C1s XPS spectrum in Fig. 1c suggests the presence of three chemical distinct species, namely C-C (284.6 eV), C-N or C-O (286.0 eV) and C=O (288.7 eV).[17] The presence of C-O and C=O in the carbon-based composites always could be observed for the metal nitrides/carbon materials.[18] As shown in Fig. 1d, the N1s XPS spectrum could be deconvoluted into three types of N species, corresponding with N-Cr at 396.4 eV, pyridinic-N at 398.3 eV and graphitic-N at 400.4 eV, respectively,[19,20,21] all of which are considered to be favorable for ORR. The existence of graphitic-N demonstrates that N is also doped into GC and the carbon nitrides could be formed. XPS in Fig. S4 shows the GC contained certain amount of N-dopant, where it can be seen that graphitic-N was the dominated specie, demonstrating the formation of carbon nitrides. It is further indicated that the carbon nitrides in the hybrid is beneficial to the ORR performance. The inductively coupled plasma−atomic emission spectrometry (ICP-AES) and elemental analyses were used for further determining the chemical composition of the synthetic catalysts. As shown in Table S3, the formulas of the carbon nitrides in CrN/GC-2-900 and GC are $CN_{0.016}$ and $CN_{0.014}$, respectively. The average domain size of ordered carbon nitride could be evaluated on the basis of the ratio between the peak areas under the D-band and G-band. Thus, the size of the crystalline domains in CrN/GC-2-900 and GC are about 0.77 and 0.80 nm (Table S4), respectively. Notably, there is almost no iron could be detected, indicating the completely removal of iron species by treating with treating with hydrochloric acid. The Brunauer-Emmett-Teller (BET) surface area of the CrN/GC-2-900 tested by the N_2 adsorption isotherm is about 165.6 $m^2 g^{-1}$ (Fig. S5), which is larger than those of the reported nitride materials.[22]

The morphology and structure of the CrN/GC-2-900 was further investigated by transmission electron microscopy (TEM). It can be seen that CrN nanoparticles (NPs) with the size of 15–30 nm are uniformly dispersed on continuous graphitic carbon nanocapsules (Fig. 2a and 2b). As shown in Fig. 2c and 2d, the high-resolution TEM (HRTEM) images clearly display that the CrN NPs are enclosed by carbon layers, ascribing from the precursor of $Cr_2O_7^{2-}$ ions would embedded into the backbone of PWAR carbon resource in the ion-exchanged process. The measured crystal lattice distance of 0.21 and 0.34 nm are attributed to the CrN (200) and graphitic carbon (002) facets, respectively, demonstrating the well crystallinity of the hybrid. The intimate contact between CrN NPs and GC makes it possible to promote the transport of electrons among them and further enhance the catalytic activity towards ORR.

The electrocatalytic activity of the synthetic hybrid was estimated by a rotating ring disk electrode (RRDE) electrode in an O_2-saturated 0.1 M KOH electrolyte with a scan rate of 5 mV s^{-1} at 1600 rpm. The synthetic GC and the commercial Pt/C (40 wt.%, JM) were also investigated for comparison. As shown in Fig. 3a, the onset potential (E_{onset}) observed at the

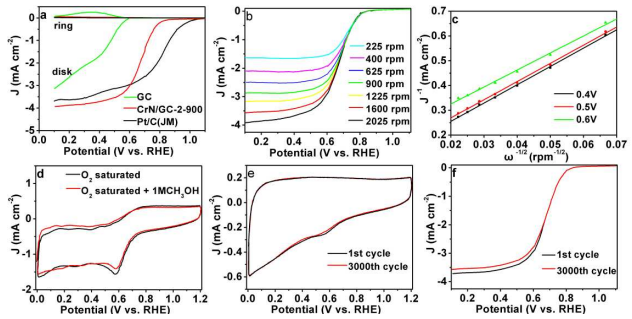

Fig.3 (a) RRDE voltammograms for the ORR in an O_2-saturated 0.1 M KOH at a scan rate of 5 mV s^{-1} at 1600 rpm. (b) LSV curves recorded for CrN/GC-2-900 electrode in an O_2-saturated 0.1 M KOH solution at the rotation rate of 225 to 2025 rpm at a scan rate of 5 mV s^{-1}; (c) is the corresponding Koutecky-Levich plot of J^{-1} vs. $\omega^{-1/2}$ at different potentials. (d) CV curves of CrN/GC-2-900 at a scan rate of 50 mV s^{-1} in O_2-saturated 0.1 M KOH electrolyte as well as O_2-saturated 0.1 M KOH+1 M CH_3OH mixture electrolyte; (e) CV curves of CrN/GC-2-900 electrode before and after 3000 cycles at a scan rate of 50 mV s^{-1} in N_2-saturated 0.1 M KOH electrolyte; (f) LSV curves of CrN/GC-2-900 electrolyte before and after 3000 cycles in O_2-saturated 0.1 M KOH electrolyte at a scan rate of 5 mV s^{-1} at 1600 rpm.

current cut-off of –0.0050 mA cm^{-2} for CrN/GC-2-900 electrode is about 0.86 V (vs. RHE), which is much more positive than that of the GC (0.59 V vs. RHE), indicating the CrN/GC-2-900 exhibits higher activity towards ORR. Notably, the E_{onset} for CrN/GC-2-900 electrode is negative shift compared with that of the Pt/C electrode (0.98 V vs. RHE), but the corresponding diffusion limiting current density (i_L) is higher than that of the Pt/C electrode when the potential is below 0.6 V (vs. RHE), demonstrating the CrN/GC-2-900 with more active sites that would be favourable for incoming more oxygen. To compare the catalysts' intrinsic activity, the corresponding Tafel plots are shown in Fig. S6. The smaller Tafel slope of the CrN/GC-2-900 (85.2 mV $decade^{-1}$) than that of the Pt/C (116.3 mV $decade^{-1}$) indicates the excellent ORR performance of CrN/GC-2-900 catalyst. In comparison, the CrN/GC hybrids with different CrN content and different heating treatment temperatures were also prepared. The corresponding characterizations about the CrN content and structures of the hybrids were displayed in Table S2, Table S4, Fig. S2, Fig. S7 and Fig. S8. Compared with the other CrN/GC hybrids, the CrN/GC-2-900 displays a superior ORR activity with more positive reduction peak potential, onset potential, and higher i_L (see Fig. S9 and Table S5). It is suggested that the high ORR performance of the CrN/GC-2-900 might be the results of the collective action of CrN and GC in the hybrid, the Pt-like property of CrN, the appropriate crystallinity, and the moderate content of CrN.

The ORR mechanism occurred on the electrode was tested by linear sweep voltammogram (LSV) curves at different rotation speeds (Fig. 3b), and the corresponding Koutckey-Levich (K-L) plots were shown in Fig. 3c. It can be observed that the CrN/GC-2-900 electrode exhibits good linearity K-L plots in the range of 0.40~ 0.60 V (vs. RHE) as the same as the Pt/C electrode (see Fig. S10), suggesting the first order reaction kinetics toward the concentration of O_2.[23] The electron transfer number (n) is calculated on the basis of the ring and disk currents (detailed calculation process displayed in supporting information). The n value for CrN/GC-2-900 is 4.10 at the potential 0.7 V (vs. RHE), thereby indicating a more efficient $4e^-$ dominated ORR process with a performance approaching that of Pt/C catalysts (3.98). The intrinsic properties of the CrN/GC-2-900 hybrid could be attributed to the synergetic effect of CrN and GC, together with the high specific surface area and the moderate CrN content, which endows the hybrid a high ORR performance.

For commercial applications, apart from high electrocatalytic activity, an ideal ORR catalyst should be able to suffer the crossover of methanol molecules from anode to cathode. As shown in Fig. 3d, there is almost no change in the ORR peak current for the CrN/GC-2-900 after the addition of methanol, whereas the Pt/C catalyst shows the typical inverse methanol oxidation peaks in CVs (see Fig. S11). The results suggest that CrN/GC-2-900 has much better crossover of methanol than Pt/C catalyst. Catalytic stability is another significant factor of FCs catalysts that needs considering in practical applications. The CrN/GC-2-900 electrode shows almost no electrochemical charateristic change and no ORR potential shift after 3000 cycles (Fig. 3e and 3f), while ECSA of the Pt/C electrode loss quickly and a nearly 50 mV half-wave potential negative shift was obtained under the same conditions (Fig. S12), suggesting a superior cyclic stability of the CrN/GC-2-900 hybrid. The chronoamperometric measurements over 10000 s were shown in Fig. S13. Notably, the CrN/GC-2-900 catalyst could keep 95.7 % of its initial current density after test, which is much higher than that of Pt/C catalysts (only 70.1 % residual). The results further demonstrate the better durability of the CrN/GC-2-900 hybrid compared with the Pt/C catalyst. Such excellent durability of the hybrid is of greatest importance for the future application of FCs. To clarify the stability of chromium in CrN, the electrolytes after stability tests (Fig. 3f and Fig. S13) were also tested by CVs (Fig. S14) and ICP-AES, and there is no oxidation/reduction about Cr^{2+}/Cr^{3+} and no Cr species could be detected. The above analyses further demonstrate the chromium in the CrN in indeed very stable. The synthetic CrN/GC hybrid exhibits much higher ORR performance (higher E_{onset} and stability) than the reported Fe-N supported on graphitic carbon, mesoporous carbon or graphene catalysts.[24-26] Therefore, our present study provides a high performance Pt-free catalyst for ORR.

In Conclusion, the CrN/GC hybrid had been successfully synthesized through a solvothermal-assisted ion-exchanged route. The synthetic hybrid composed of 20 nm CrN NPs uniformly supported on GC containing carbon nitrides. As Pt-free catalyst, the CrN/GC-2-900 hybrid exhibits high activity, excellent tolerance to methanol, outstanding stability and a four-electron reduction pathway towards ORR. The excellent performance should be attributed to the Pt-like property of CrN, the intimate contact between CrN and GC benefits to the development of the synergistic effect for ORR, meanwhile, the existence of carbon nitrides in the hybrid can expose more active sites. The superior performances and low-cost of the CrN/GC-2-900 hybrid make it a promising candidate to replace Pt in FCs.

Acknowledgements

We gratefully acknowledge the support of this research by the National Natural Science Foundation of China (21371053, 21401048), the Cultivation Fund of the Key Scientific and Technical Innovation Project, the Ministry of Education of China (708029), the China Postdoctoral Science Foundation (2014M551285), the Postdoctoral Science Foundation of Heilongjiang Province (LBH-TZ0519), the Natural Science Foundation of Heilongjiang Province (QC2014C007), Innovative Research Project of Key Laboratory of Functional Inorganic Material Chemistry, Ministry of Education

Notes and references

1 H. A. Gasteiger and N. M. Markovic, *Science*, 2009, **324**, 48.
2 M. K. Debe, *Nature*, 2012, **486**, 43.
3 L. Li and Z. Wei, Chem. *Soc. Rev.*, 2015,**44**, 2168.
4 Y. Wang, N. Zhao, B. Fang, H. Li, X. T. Bi and H. Wang, *Chem. Rev.*, 2015, **115**, 3433.
5 Z. Chen, D. Higgins, A. Yu, L. Zhang and J. Zhang, *Energy Environ. Sci.*, 2011, **4**, 3167.
6 R. P. Singh, E. J. Bae and J. Yu, *J. Am. Chem. Soc.*, 2015, **137**, 3165.
7 T. Y. Ma, J. Ran, S. Dai, M. Jaroniec and S. Z. Qiao, *Angew. Chem. Int. Ed.,* 2015, **54**, 4646.
8 V. D. Noto, E. Negro, S. Polizzi, F. Agresti and G. A. Giffin, *ChemSusChem*, 2012, **5**, 2451.
9 E. Negro, K. Vezzù, F. Bertasi, P. Schiavuta, L. Toniolo, S. Polizzi and V. D. Noto, *ChemElectroChem*, 2014, **1**, 1359.
10 V. Di Noto, E. Negro, S. Polizzi, K. Vezzù, L. Toniolo and G. Cavinato, *Int. J. Hydrogen Energy*, 2014, **39**, 2812.
11 E. Negro, S. Polizzi, K. Vezzù, L. Toniolo, G. Cavinato and V. Di Noto, *Int. J. Hydrogen Energy*, 2014, **39**, 2828.
12 G. R. Li , J. Song , G. L. Pan and X. P. Gao, *Energy Environ. Sci.*, 2011, **4**, 1680-1683.
13 L. Wang, J. Yin, L. Zhao, C. Tian, P. Yu, J. Wang and H. Fu, *Chem. Commun.*, 2013, **49**, 3022.
14 M. Yang, R. Guarecuco and F. J. DiSalvo, *Chem. Mater.*, 2013, **25**, 1783.
15 Y. Shi, Y. Wan, R. Zhang and D. Zhao, *Adv. Funct. Mater.,* 2008, **18**, 2436.
16 M. Chen, S. Wang, J. Zhang, D. He and Y. Zhao, *Chem. Eur. J.*, 2012, **18**, 15459.
17 X. Zhang, D. Liu, L. Li and T. You, *Sci. Rep.*, 2015, **5**, 9885.
18 J. Yin, L. Wang, C. Tian, T. Tan, G. Mu, L. Zhao and H. Fu, *Chem. Eur. J.*, 2013, **19**, 13979.
19 F. Rivadulla, M. Bañobre-López, C. X. Quintela, A. Piñeiro, V. Pardo, D. Baldomir, M. A. López-Quintela, J. Rivas, C. A. Ramos, H. Salva, J. S. Zhou and J. B. Goodenough, *Nat. Mater.*, 2009, **8**, 947.
20 G. Nam, J. Park, S. T. Kim, D. Shin, N. Park, Y. Kim, J. Lee and J. Cho, *Nano Lett.*, 2014, **14**, 1870.
21 J. Sanetuntikul, T. Hang and S. Shanmugam, *Chem. Commun.*, 2014, **50**, 9473.
22 Z. Pan, Y. Xiao, Z. Fu, G. Zhan, S. Wu, C. Xiao, G. Hua and Z. We, *J. Mater. Chem. A*, 2014, **2**, 13966.
23 W. Niu, L. Li, X. Liu, N. Wang, J. Liu, W. Zhou, Z. Tang and S. Chen, *J. Am. Chem. Soc.*, 2015, **137**, 5555.
24 H.-W. Liang, W. Wei, Z.-S. Wu, X. Feng and K. Müllen, *J. Am. Chem. Soc.*, 2013, **135**, 16002.
25 Y. Zhang, K. Fugane, T. Mori, L. Niu and J. Ye, *J. Mater. Chem.*, 2012, **22**, 6575.
26 E. Negro, A. H. A. M. Videla, V. Baglio, A. S. Aricò, S. Specchia and G. J. M. Koper, *Appl. Catal. B: Environmental*, 2015, **166–167**, 75.